**Supporting Information**

**A three-dimensionally stretchable high performance supercapacitor**

*Sisi He,[a] Longbin Qiu,[a] Lie Wang,[a] Jingyu Cao,[a] Songlin Xie,[a] Qiang Gao,[ab] Zhitao Zhang,[a] Jing Zhang,[a] Bingjie Wang\*[a] and Huisheng Peng\*[a]*
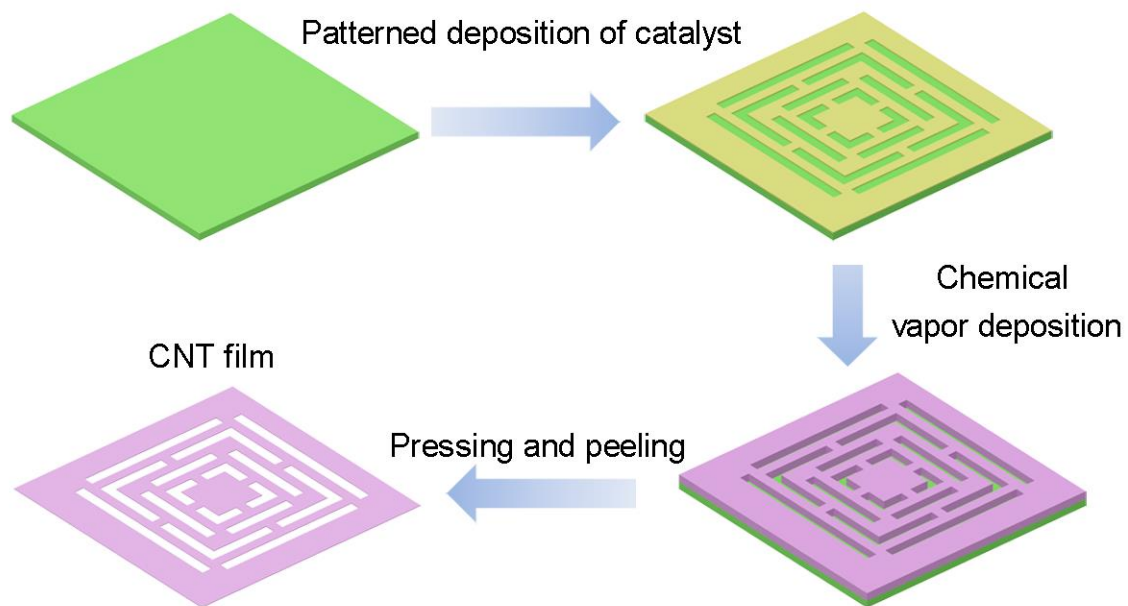
[a]*State Key Laboratory of Molecular Engineering of Polymers, Department of Macromolecular Science and Laboratory of Advanced Materials, Fudan University, Shanghai 200438, China; E-mail: penghs@fudan.edu.cn.*

[b]*Key Laboratory of Science and Technology of Eco-Textiles, Ministry of Education, Jiangnan University, Wuxi 214122, China*

**Experimental section**

*Characterization.* The structures were characterized by scanning electron microscopy (SEM) (Hitachi FE-SEM S-4800) and transmission electron microscope (TEM) (JEOL JEM-2100F). The photographs were taken by a digital camera (Nikon, J1). The electrical conductivities were measured by Keithley Model 2400 Source Meter. The thicknesses were obtained using a surface profiler (Veeco, Dektak 150). The weight of the carbon nanotube (CNT) film was measured by using a microbalance (Sartarious SE2). The oxygen plasma treatment was performed in an oxygen microwave (Plasma System 690, PVA Tepla). Galvanostatic charge-discharge curves and cyclic voltammograms were conducted at an electrochemical workstation (CHI 660D). Cyclic galvanostatic charge-discharge measurements were characterized from an ARBIN electrochemical station (MSTAT-5 V/10 mA/16 Ch).

*Calculation of electrochemical parameters of supercapacitors.* The areal capacitance ($C_A$), gravimetric capacitance ($C_M$) and volumetric capacitance ($C_V$) are calculated by the following equations: $C_A = 2 \times I \times \Delta t/(S \times U)$, $C_V = 2 \times I \times \Delta t/(V \times U)$ and $C_M = 2 \times I \times \Delta t/(m \times U)$. Here $I$, $\Delta t$ and $U$ are discharge current, discharge time and voltage window, respectively. $S$, $m$ and $V$ are the total surface area, mass and volume of the electrode, respectively. In this work, $m$ was measured by using a microbalance, typically 0.619 mg for a CNT film with an area of 0.36 cm$^2$. The volume of the electrode can be obtained by $V = L \times W \times H$, where $L$, $W$ and $H$ represent the length, width and thickness of the CNT film, respectively. In a symmetrical supercapacitor, the specific capacitance of supercapcaitor $Cs = 0.25 \times C_E$ where $C_E$ is the capacitance of a single electrode. The volumetric energy density ($E_V$) and volumetric power density ($P_V$) of the supercapacitor can be expressed as: $E_V = 0.5 \times C_S \times U^2 = 0.125 \times C_V \times U^2$ and $P_V = E_V \times 3600/\Delta t$.

Patterned deposition of catalyst

Chemical
vapor deposition

CNT film

Pressing and peeling

**Figure S1.** Schematic illustration to the preparation of a pyramid-shaped CNT film. The preparation included the selected deposition of catalyst and growth of aligned CNT array, followed by pressing and peeling to obtain the desired CNT film.
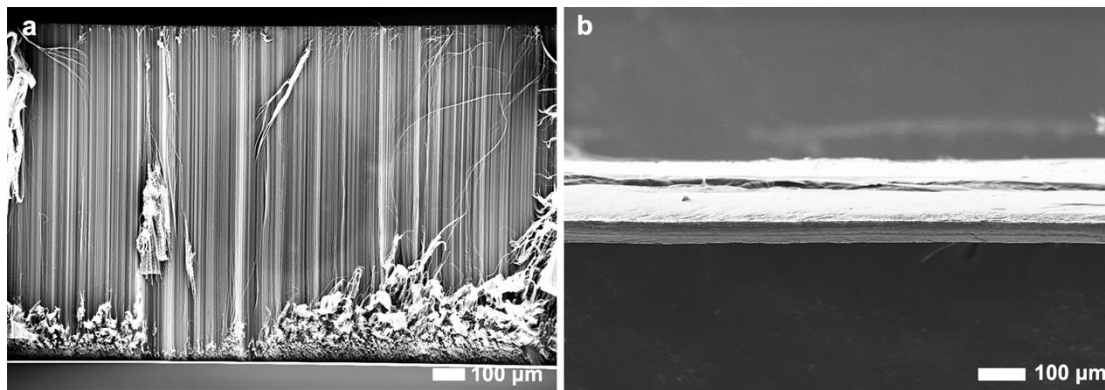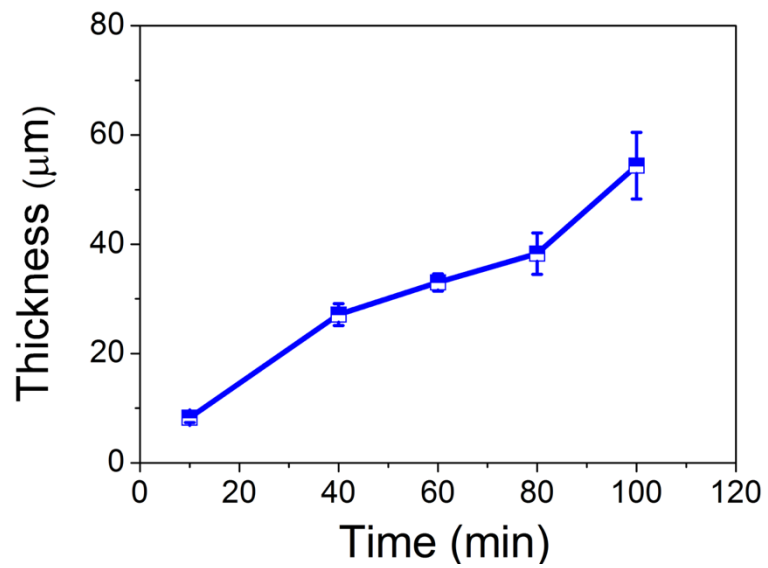
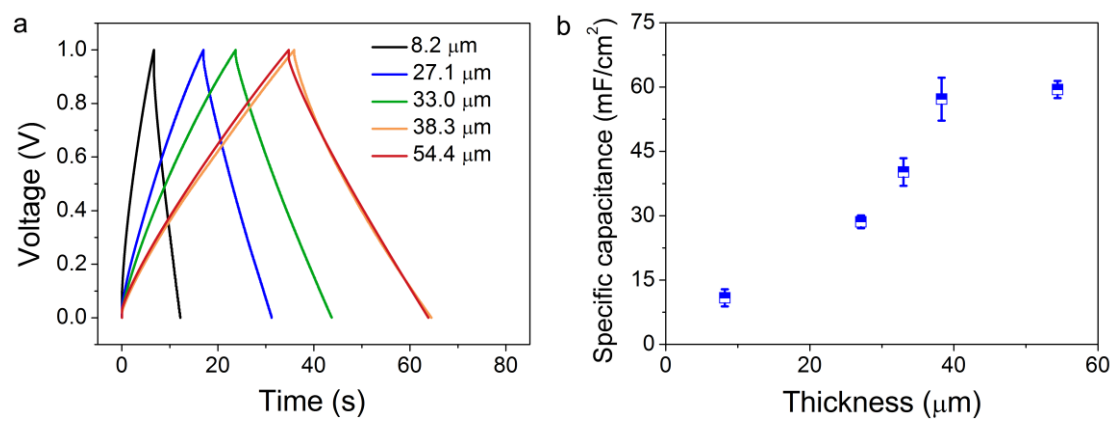**Figure S2**. SEM images of the CNT array before **(a)** and after pressing **(b)**.
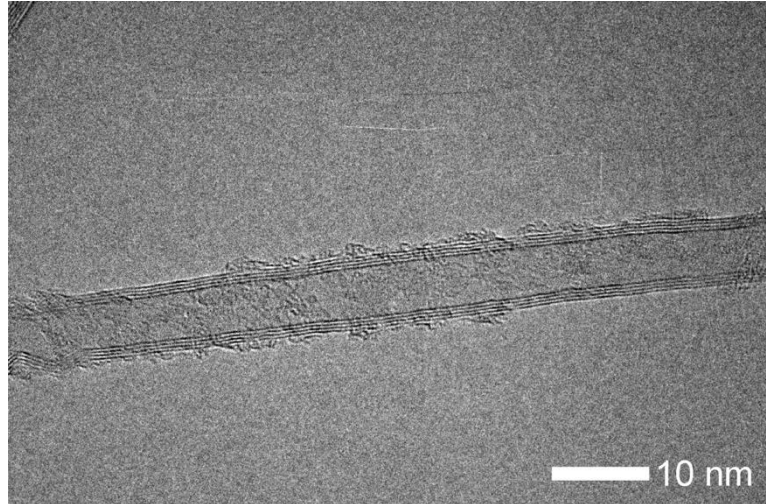
**Figure S3.** TEM image of a CNT.
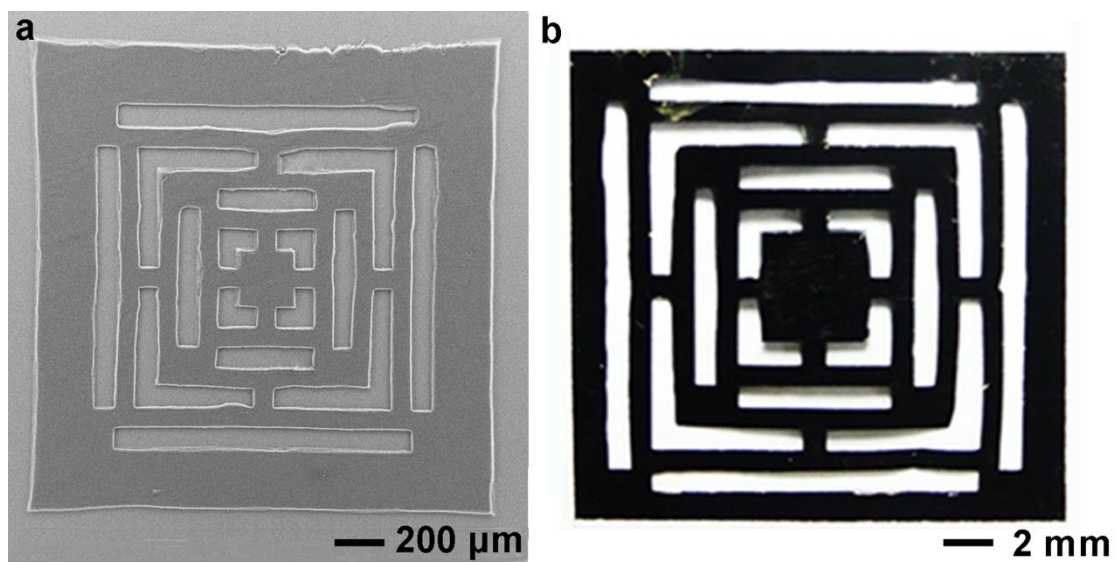
**Figure S4. (a)** SEM image of a pyramid-shaped CNT film with widths of millimeters. **(b)** Photograph of a pyramid-shaped CNT film with widths of centimeters.
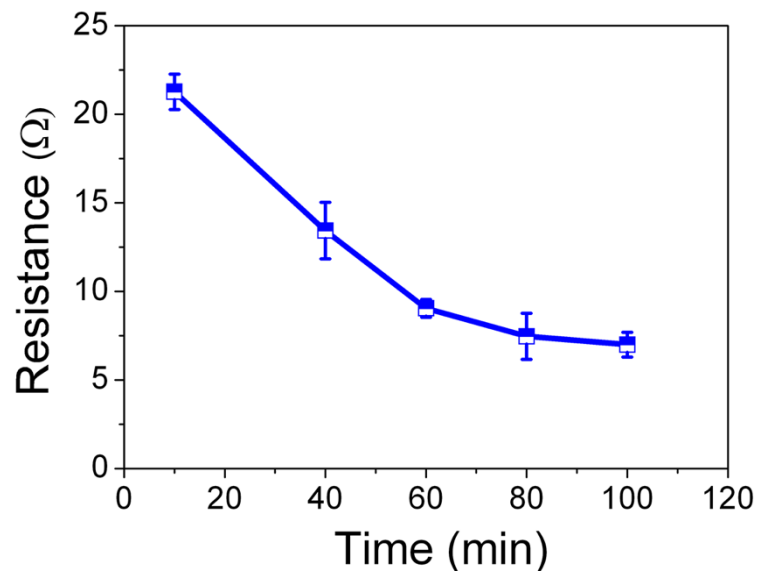
**Figure S5**. Dependence of the CNT film thickness (after pressing) on the growth time.

**Figure S6. (a)** Galvanostatic charge-discharge profiles with increasing thicknesses of the CNT film electrodes at the current density of 1 mA/cm$^2$. **(b)** Dependence of the specific capacitance on the CNT thickness.
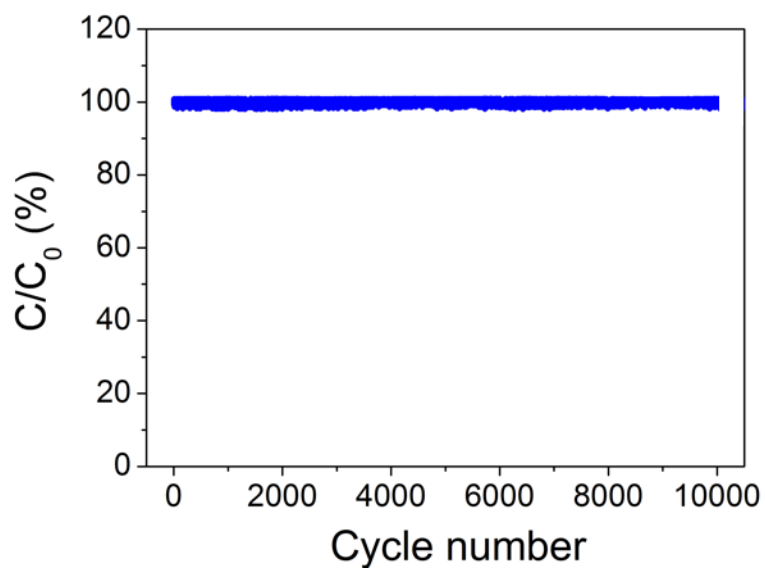
**Figure S7.** Dependence of the resistance of CNT film on the growth time. The CNT films shared a width of 2 mm and length of 5 mm.
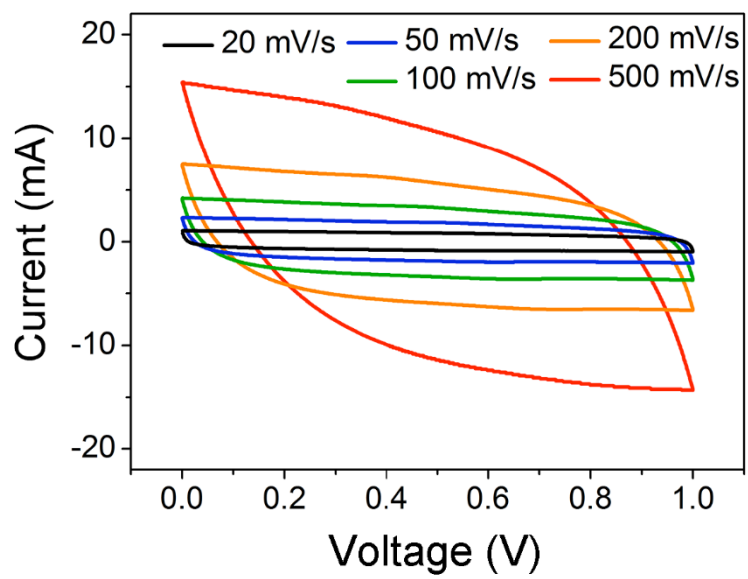
**Figure S8.** Cyclic voltammograms at increasing scan rates from 20 to 500 mV/s.

**Figure S9.** Dependence of the specific capacitance on the cycle number at a current density of 1 A/cm$^2$. Here $C_0$ and $C$ correspond to specific capacitances before and after cycling, respectively.

**a**



**b**
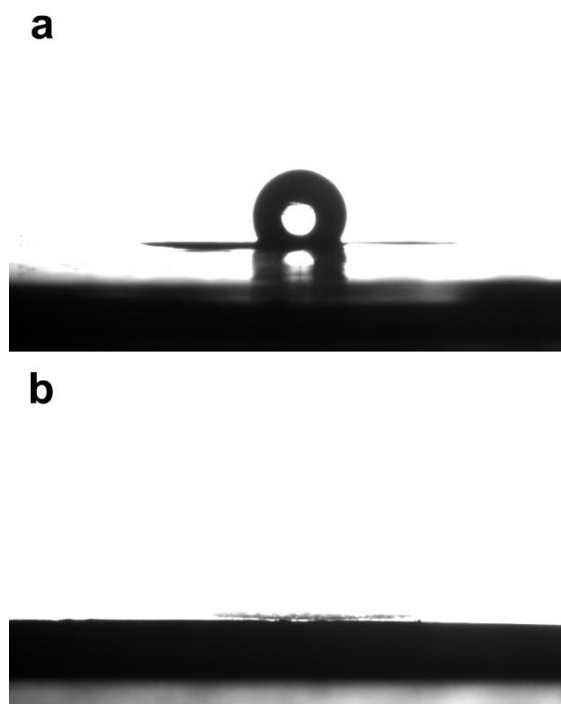


**Figure S10.** The surface properties of a CNT film before and after oxygen plasma treatment. **(a)** Hydrophobic. **(b)** Hydrophilic.
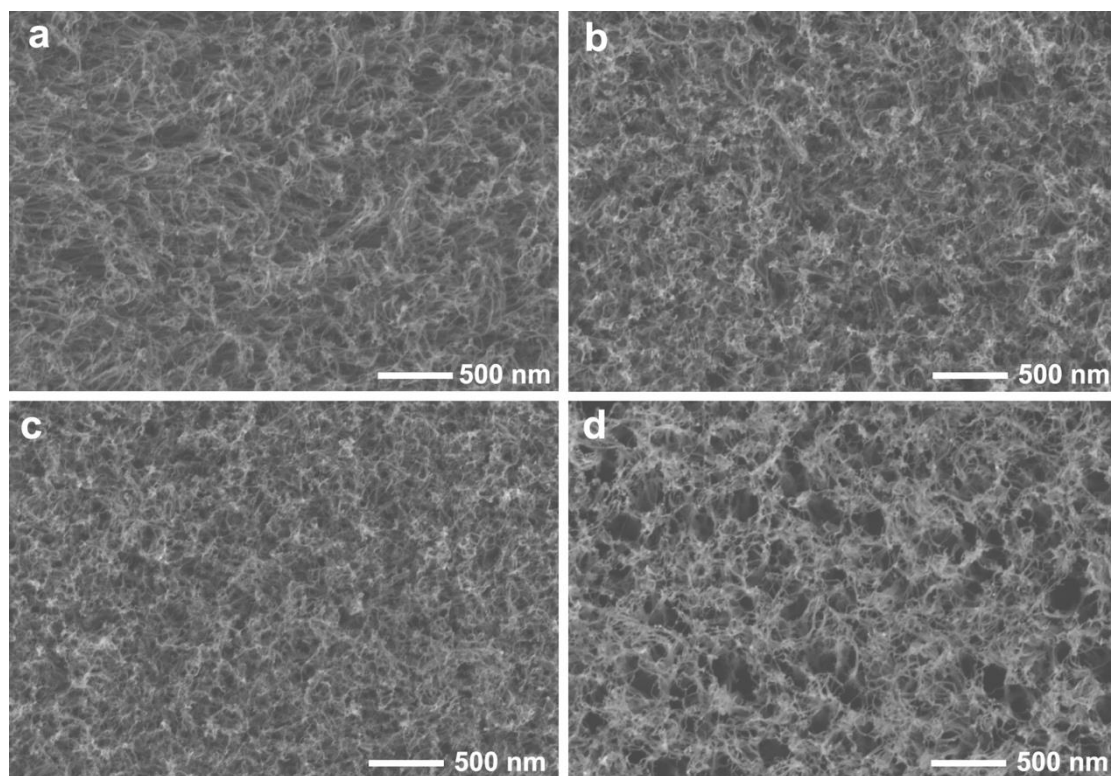
**Figure S11.** Surface morphologies of CNT films after oxygen plasma treatment with increasing oxygen contents. **(a)** 5.29 wt%. **(b)** 6.67 wt%. **(c)** 8.26 wt%. **(d)** 9.27 wt%.
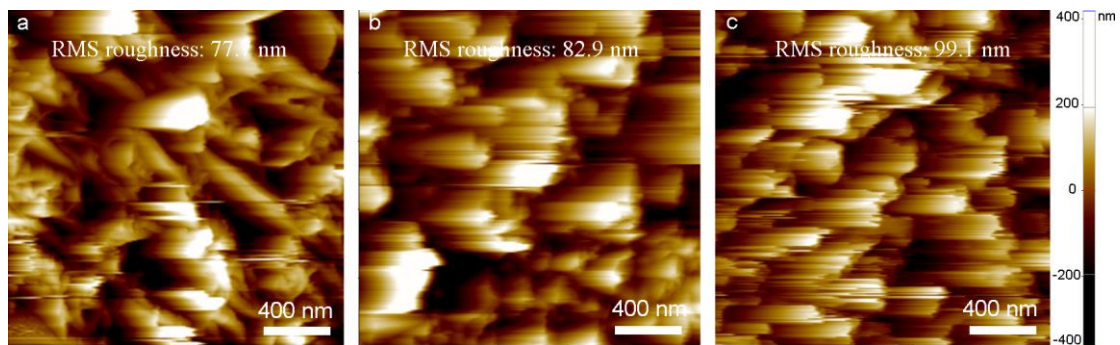
**Figure S12.** AFM images of the CNT films after oxygen plasma treatment with increasing oxygen contents with the primary film as a comparison. **(a)** 3.06 wt%, **(b)** 5.29 wt% and **(c)** 9.27 wt%.
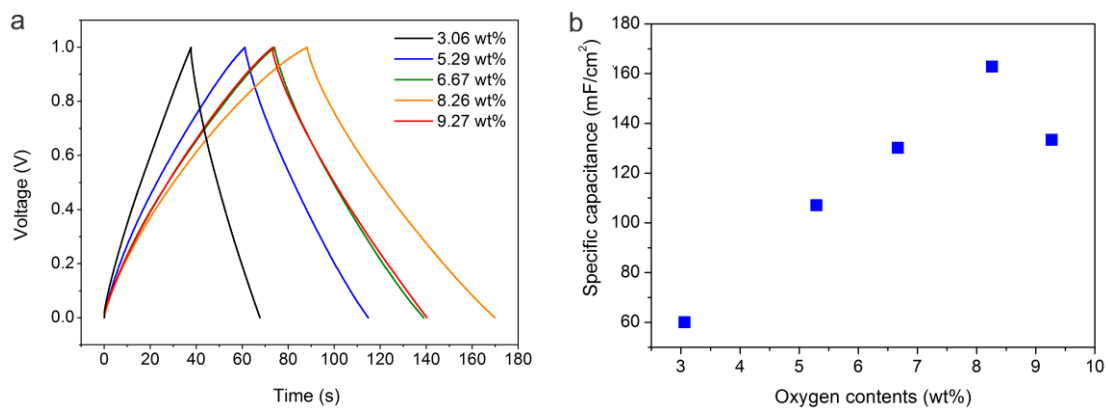
**Figure S13. (a)** Galvanostatic charge-discharge profiles at increasing oxygen contents.
**(b)** Dependence of the specific capacitance on the oxygen content.
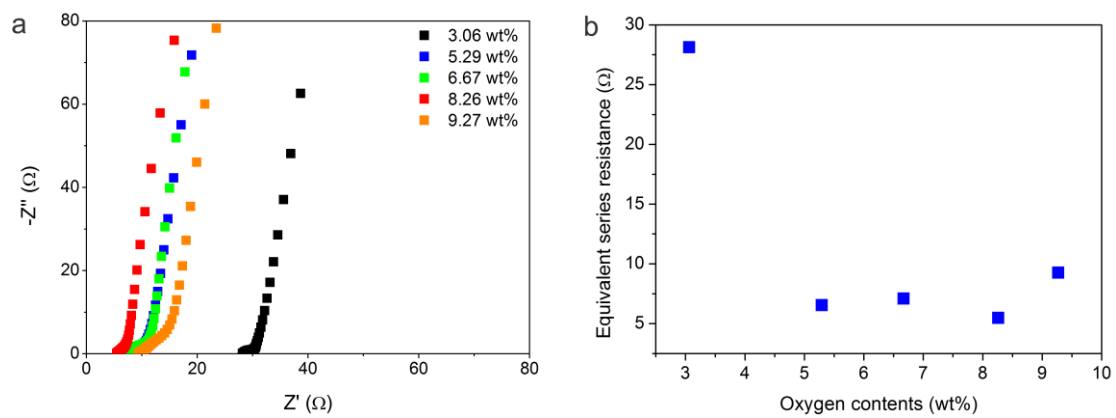
**Figure S14. (a)** Nyquist plots of the supercapacitors fabricated from CNT films with increasing oxygen contents. **(b)** The equivalent series resistance of the supercapacitors fabricated from CNT films with increasing oxygen contents.
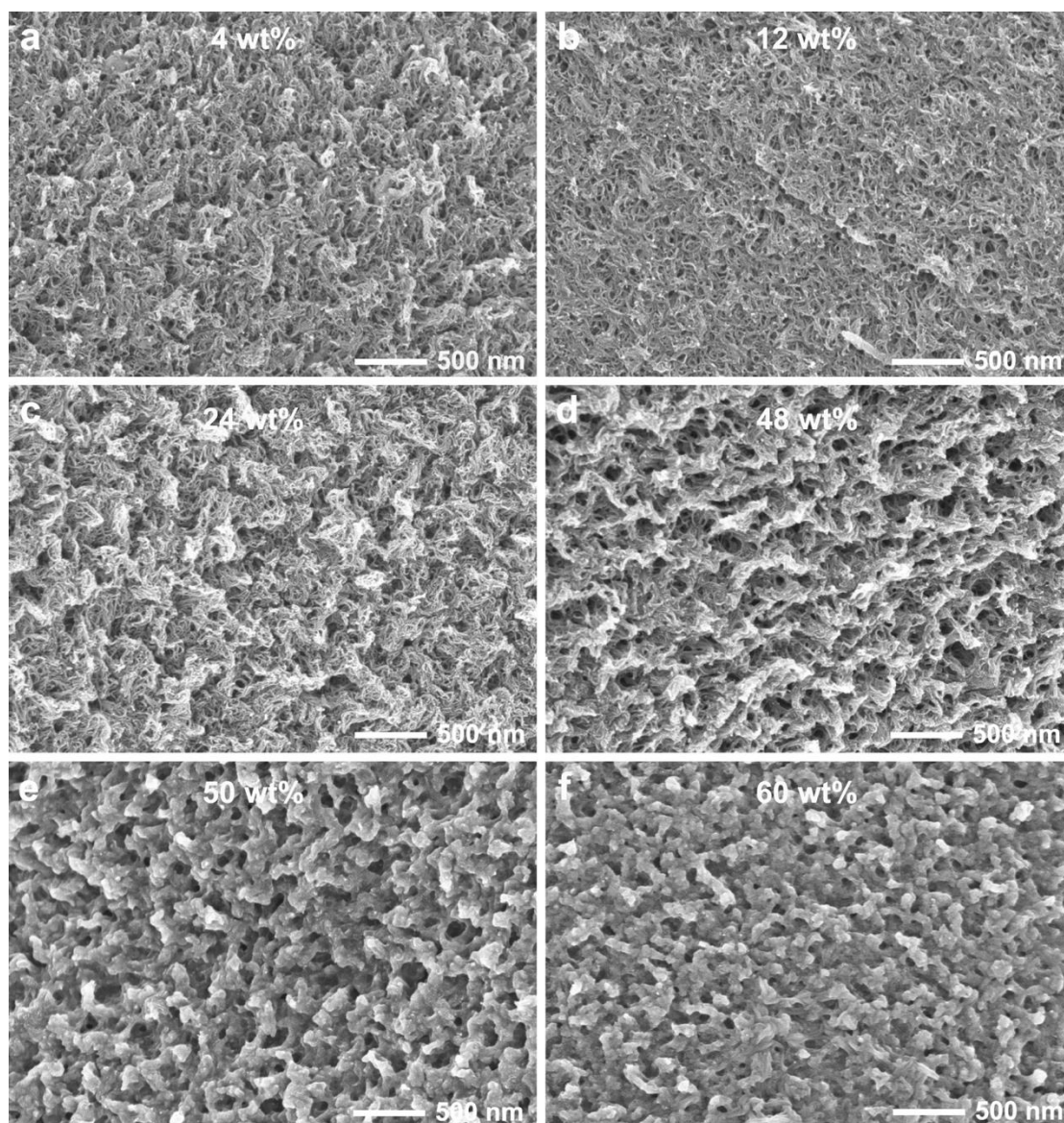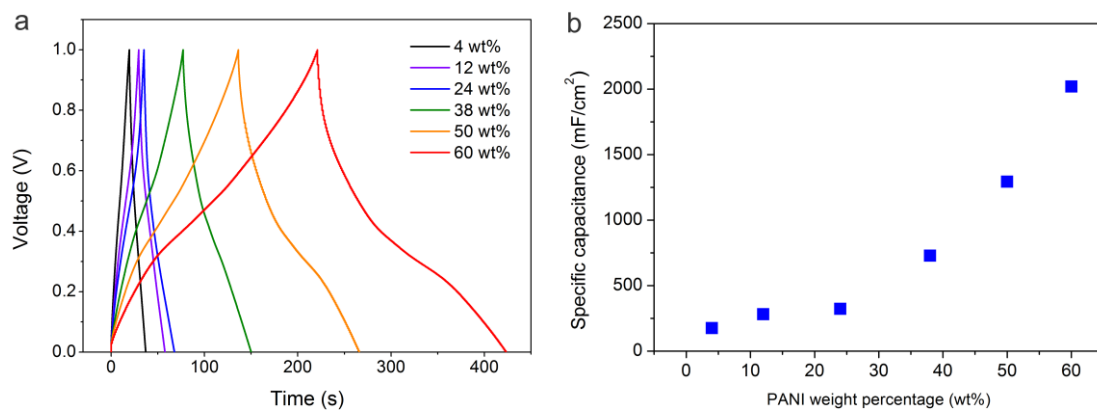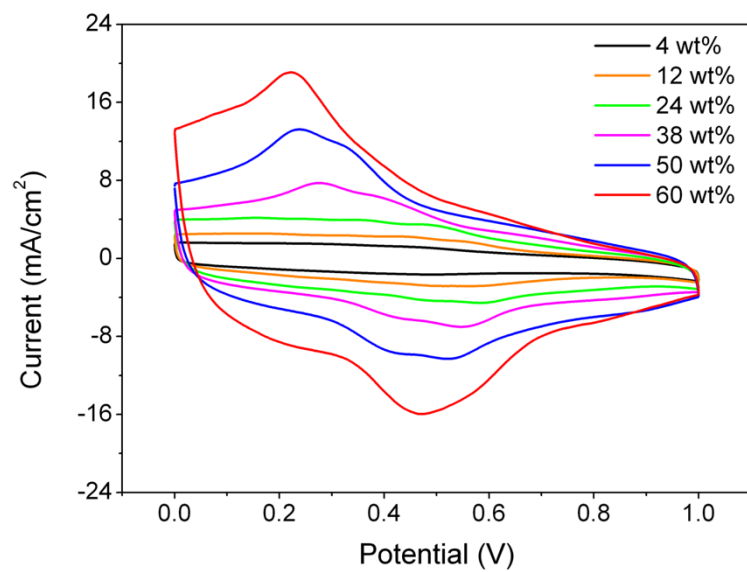
**Figure S15.** SEM images of the CNT/PANI composite films with increasing PANI weight contents from 4 wt% **(a)**, 12 wt% **(b)**, 24 wt% **(c)**, 48 wt% **(d)**, and 50 wt% **(e)** to 60 wt% **(f)**.
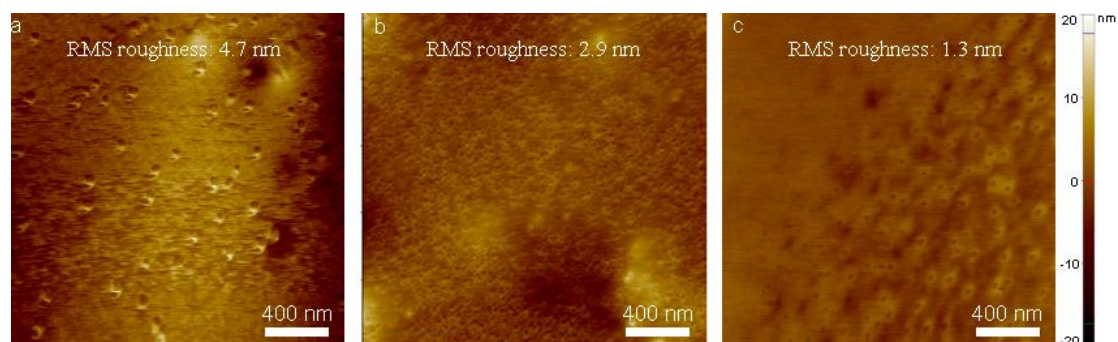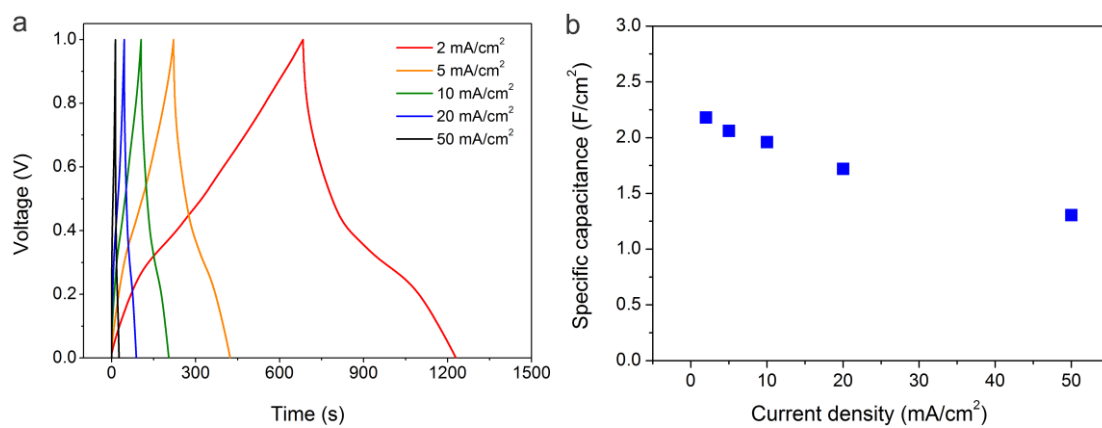
**Figure S16.** AFM images of the CNT/PANI composite films with increasing PANI weight contents. **(a)** 4 wt%, **(b)** 48 wt% and **(c)** 60 wt%.

**Figure S17. (a)** Galvanostatic charge-discharge profiles at increasing PANI weight percentages. **(b)** Dependence of the special capacitance on the PANI weight percentage.

**Figure S18.** Cyclic voltammograms at increasing PANI weight percentages.

**Figure S19.** (**a**) Galvanostatic charge-discharge profiles of the supercapacitor from the CNT/PANI composite film electrode (60 wt% PANI) at increasing current densities. (**b**) Dependence of the specific capacitance on the current density.
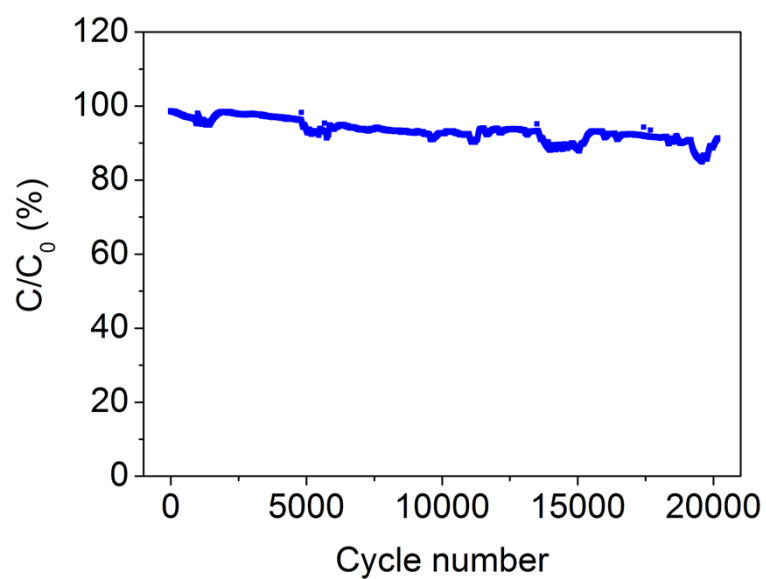
**Figure S20.** Dependence of the specific capacitance on the cycle number at a current of 1 mA. Here $C_0$ and C correspond to specific capacitances before and after cycling, respectively.

**Table S1.** Oxygen contents of CNT films as verified by energy-dispersive X-ray spectra after oxygen plasma treatment with increasing times.

| Treatment time | C/wt% | O/wt% |
| --- | --- | --- |
| 0 | 96.94 | 3.06 |
| 1 | 94.71 | 5.29 |
| 2 | 93.33 | 6.67 |
| 5 | 91.74 | 8.26 |
| 10 | 90.73 | 9.27 |